HyMARC Core Activity: Metal Hydrides

HyMARC
Hydrogen Materials Advanced Research Consortium

Enabling twice the energy density for onboard H_2 storage

Mark D. Allendorf, Sandia National Laboratories (Task Lead)

NREL NATIONAL RENEWABLE ENERGY LABORATORY · Sandia National Laboratories · Lawrence Livermore National Laboratory · Berkeley Lab · Pacific Northwest National Laboratory · NIST · SLAC National Accelerator Laboratory





This presentation does not contain any proprietary, confidential, or otherwise restricted information

Project ID: ST203

Task 2: Metal Hydrides

	Focus Area project	DOE Targets: Grav. Capacity	Vol. Capacity	Fill time	Time to full flow	Min. Deliv. T	Min. Deliv. P	Cycle life	Team (lead)	Status
Surfaces & Interfaces – Thermo.	Phase diagrams: ternaries	X	X			X	X		LLNL, SNL, PNNL	Manuscript in progress
	Phase diagrams: eutectics	X	X			X	X		SNL, LLNL, PNNL,NREL	Continuing. New high-capacity eutectics in Li-Mg-B-N-H identified
	Large-scale atomistic models	X	X	X	X				SNL, LLNL	Mg-B-H forcefield completed. Extending work to unstable hydrides
	Interface Model Devel.			X	X			X	LLNL, PNNL, SNL	Continuing. MS in progress
	Surface chem & phase nucl.			X	X			X	SNL, LBNL, NREL, LLNL	Continuing. Paper *Adv. Mater. Interfaces* (2020)
Additives	B-H bond strength modulation			X	X	X			LBNL, NREL, PNNL	Continuing. Manuscript submitted.
	Additives for B-B rehydrogenation			X	X	X			SNL,LLNL,LBNL,PNNL	No-go; manuscript in prep.
	B-B/B-H catalytic activation			X	X	X			LLNL,SNL,LBNL,PNNL	No-go; manuscript in prep.
Nano strategies	Nano-MH/mechanical stress			X	X				LLNL,NREL,LBNL,PNNL	Continuing. Manuscript submitted
	Non-innocent hosts			X	X				SNL, LLNL, LBNL	Continuing. Manuscript subm. on "molecular" complex hydride
	MgB_2 nanosheets			X	X	X	X		LBNL, LLNL, SNL	Prepared nanoscale Mg-B by surfactant ball milling. Manuscript in prep.
	Microstructural impacts			X	X			X	LLNL, LBNL, SNL	Manuscript in progress
	Machine learning	X	X						SNL, LLNL	Continuing. Explainable ML applied to interstitials. Paper published in *JPCL*

Focus Area 2.B.2: Experimental probing of surface and buried interface chemistry of complex "non-ideal" systems

- **Li-N-H is fully reversible** (J. Wang *et al. MRS Bull.* 2013, 38, 480)
- **Total capacity of ~10.5 wt.% via lithium imide (Li_2NH) intermediate:**

$$Li_3N + 2\,H_2 \rightleftharpoons Li_2NH + LiH + H_2 \rightleftharpoons LiNH_2 + 2\,LiH$$

- **Model of phase evolution based on kinetic data** (B. Wood *et al. Adv. Mater. Interf.* 2017)

DFT + Wulff construction

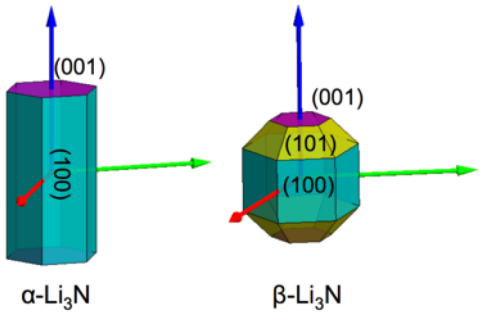

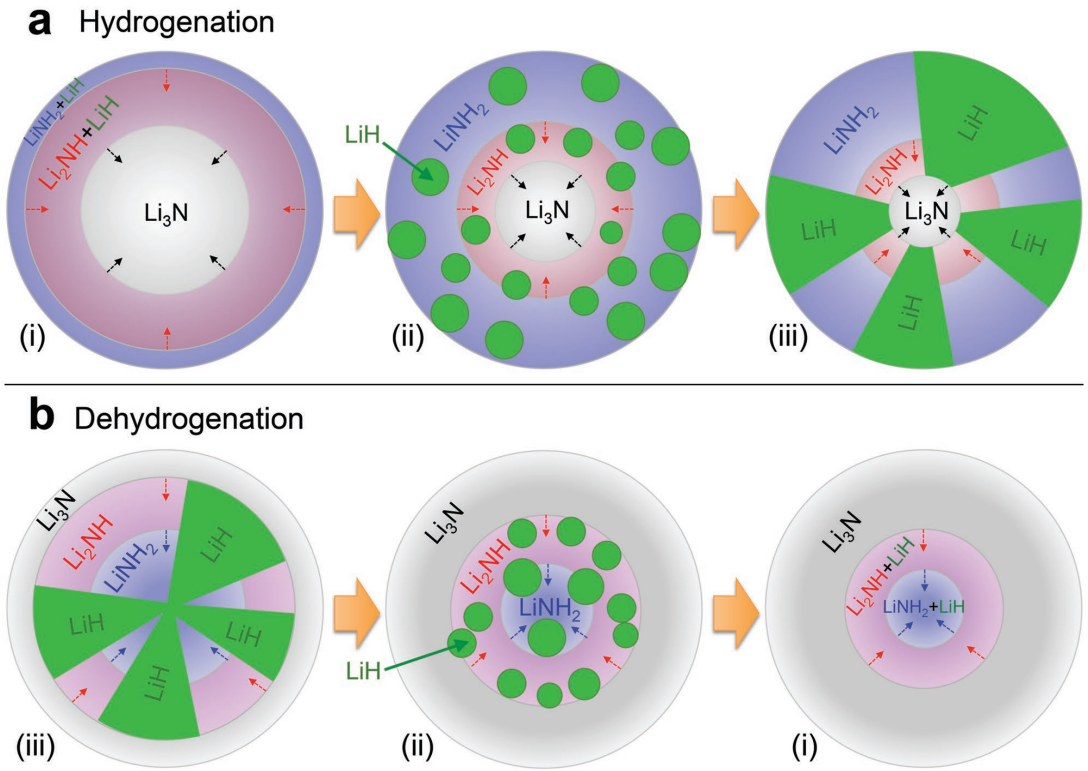

Can we image phase evolution in metal hydrides?

Uncovering the rate-limiting step in H_2 uptake/release help us design materials with kinetics that meet DOE targets for fill time

Mesoscale phase evolution (nm → μm) is commonly included in mechanisms of metal hydride chemistry, but experimental data needed for validation is lacking.

- **TEM: ineffective because hydrides decompose under electron beams**
- **Scanning transmission X-ray microscopy (STXM)**
  - Access through Approved Program at LBNL/Advanced Light Source
  - Generates **mesoscale chemical maps**
    - Beamline 5.3.2.2 allowed access only to N in this material
    - 30-nm resolution

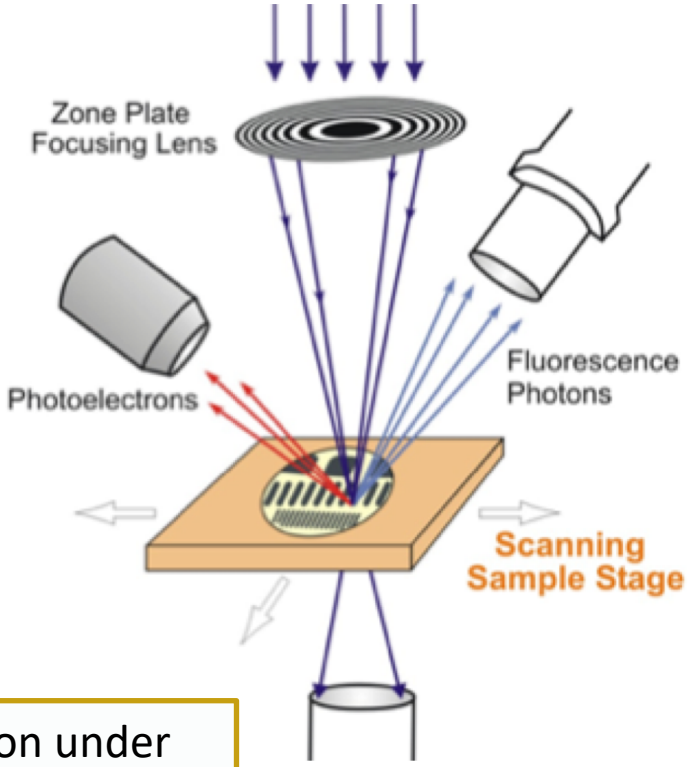

Approach: Conduct hydrogenation and dehydrogenation under realistic cycling conditions, then use clean transfer at the ALS to image at the mesoscale the reactants remaining and the products formed to understand the mechanisms of H_2 storage reactions.

STXM N K-edge maps of partially reacted $LiNH_2$+2LiH

Hydrogenation

- Reaction at 200 C
- Very little $LiNH_2$ detected

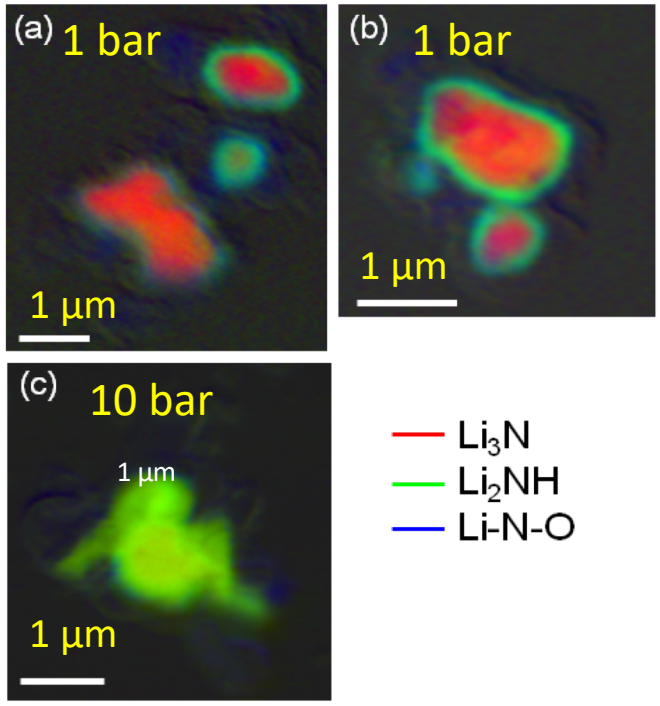

Hydrogenation: Bulk Li_3N starts to hydrogenate at the particle surface, with the imide growing into the particle center with time.

Dehydrogenation:

- 400-450 C : Interior dehydrogenates first

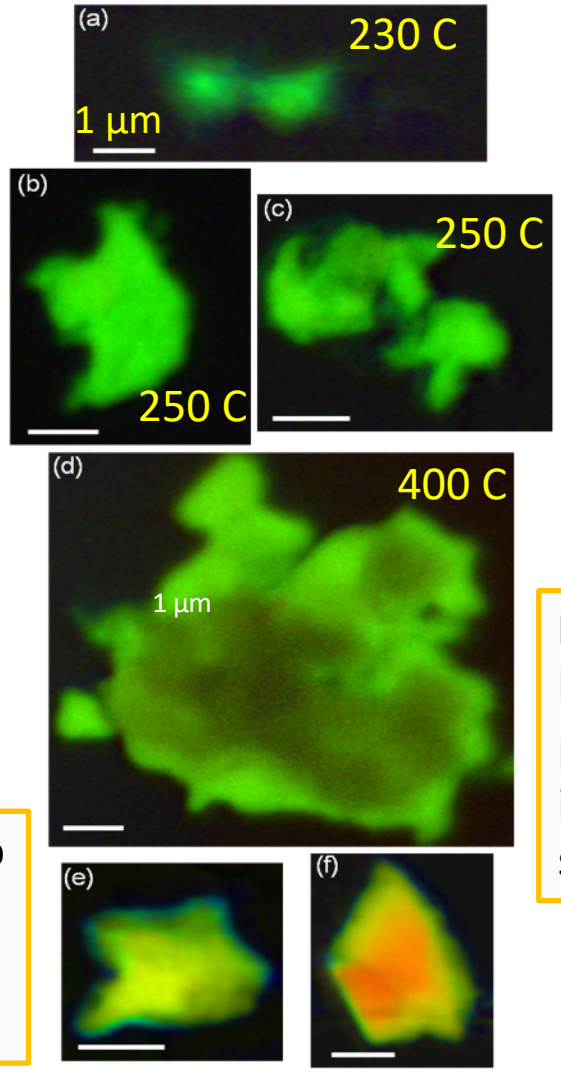

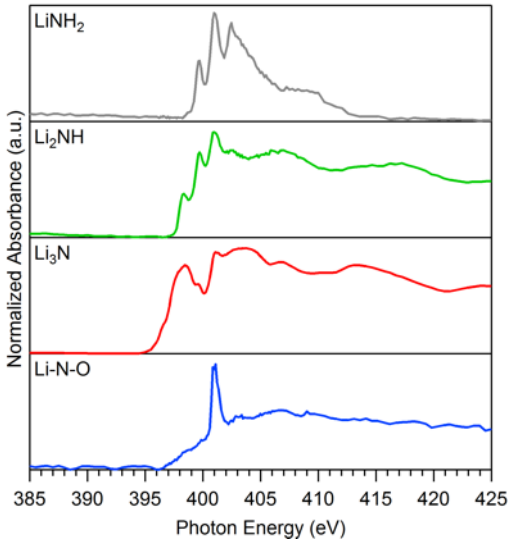

N K-edge X-ray absorption spectra, used as standards for mapping

Dehydrogenation: Bulk Li_2NH loses H from the interior of the particle first, which is counter-intuitive and currently being studied in more details.

Sandia National Laboratories

STXM maps indicate reaction is limited by the rate of H_2 release from the surface

*Hydrogenation and dehydrogenation steps for complex metal hydrides are **conducted at different temperatures and pressures**, which can lead to different rate-limiting steps.*

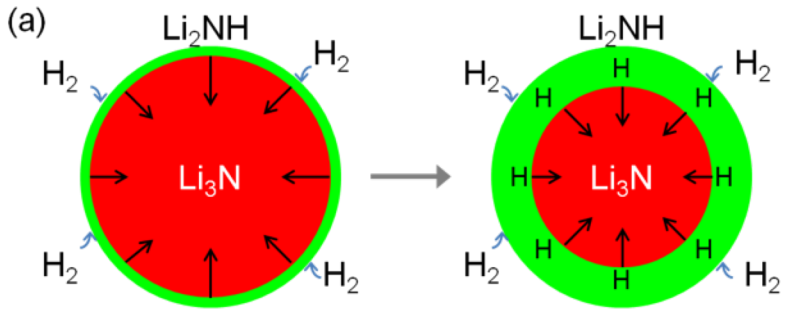

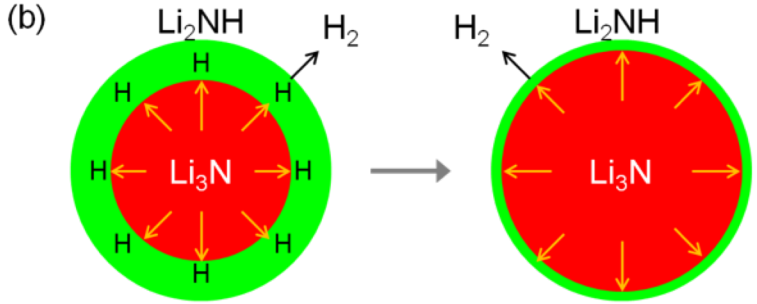

Inverted core-shell chemical map

<u>Hydrogenation</u>:

- **Proceeds as predicted by Wood et al.**

<u>Dehydrogenation</u>:

- **Slow surface kinetics lead to inverted core-shell → opposite microstructure from earlier prediction**

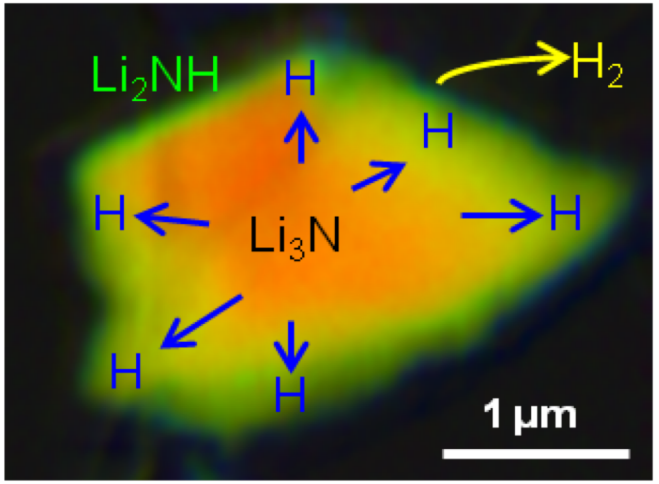

Sandia National Laboratories

Berkeley Lab

In-situ Surface Characterization of $NaAlH_4$ dehydrogenation also suggests an inverted core shell mesostructure

Finding emergent general behavior, such as inverted-core-shell dehydrogenation can improve model fidelity and provide guidance for designing, optimizing, or discarding new storage materials

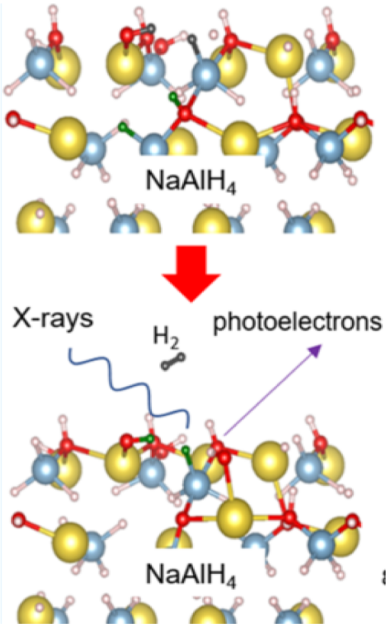

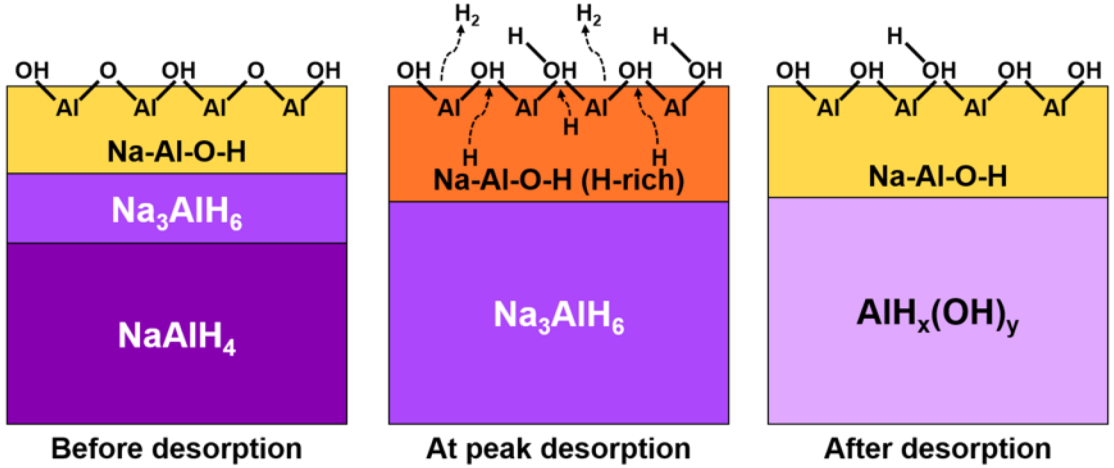

The slow surface reaction is catalyzed by activated surface Al $(OH)_x$

$$(Al - OH_2) + H \rightarrow (Al - OH) + H_2^{gas}$$

$$(Al - OH) + H \rightarrow (Al - OH_2)$$

J. L White et al. *ACS Appl. Mater. Interfaces* **11**, 4930 (2019)

Sandia National Laboratories

Complex Metal Hydrides (eutectic mixtures)

Solid-phase synthesis

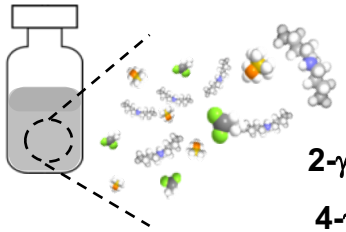

Under Ar

2-γ-MBH/$MgCl_2$ (2:8)

4-γ-MBH/$MgCl_2$ (4:6)

(weight ratio of Cl source/Mg source)

TEM images of 2-γ-MBH/$MgCl_2$

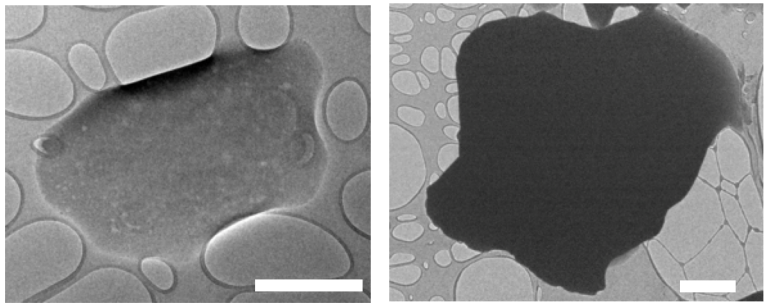

Size > 1μm

Scale bar: 500 nm

Atomic ratio

B : Cl : Mg
= 6.3 : 1.5 : 2.1

(B+Cl) : Mg = 3.7 : 1.0
*ideal : 2.0

Calculated by EDS data

XRD

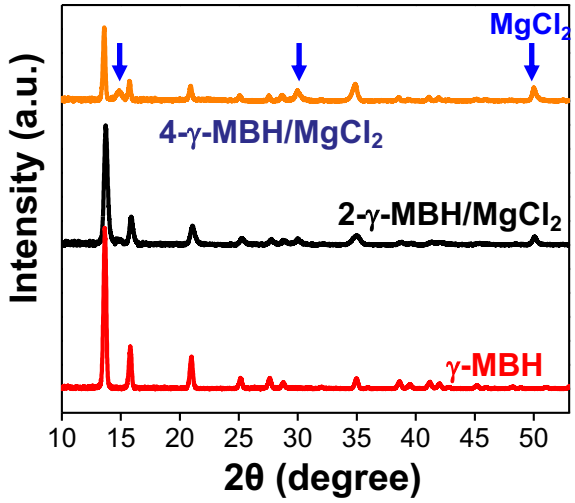

Hydrogen desorption

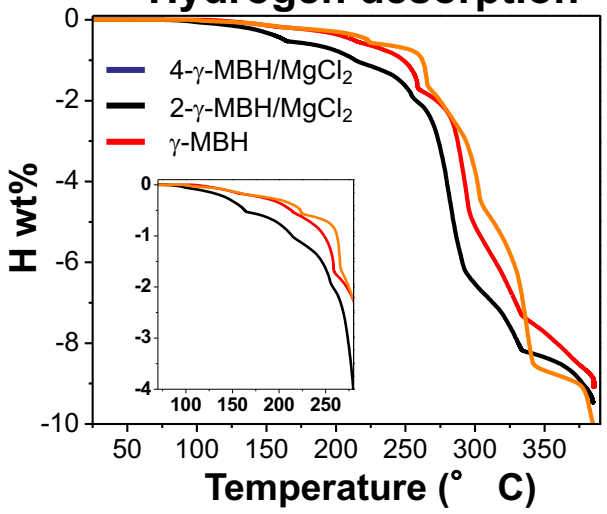

DSC

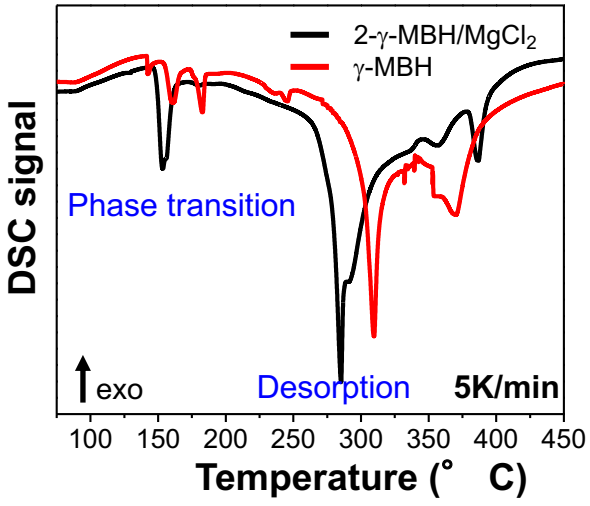

- Reducing the number of Mg cation in the mixture (perhaps by leaching Mg out to from $MgCl_2$) might lead to increase probability of BH_4 interaction and release of H_2.
- Dehydrogenation of 2-γ-MBH/$MgCl_2$ starts at lowest temperatures among them.
- Phase transition and desorption in 2-γ-MBH/$MgCl_2$ happen at lower temperature.

B and Mg K-edge of XAS in eutectic mixtures

Surface and bulk analysis in as-synthesized and dehydrogenated mixtures

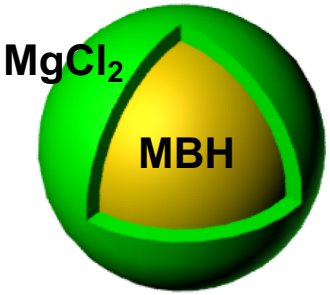

2-γ-MBH/$MgCl_2$ (2:8)

4-γ-MBH/$MgCl_2$ (4:6)

(weight ratio of Cl source/Mg source)

B K-edge of XAS

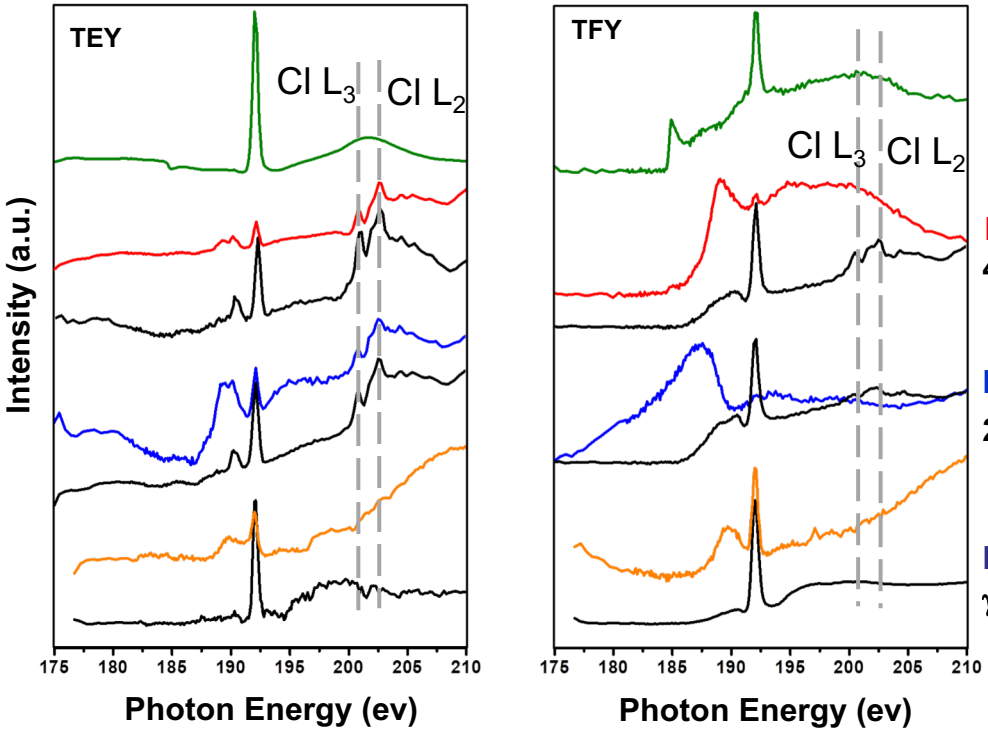

Mg K-edge of XAS

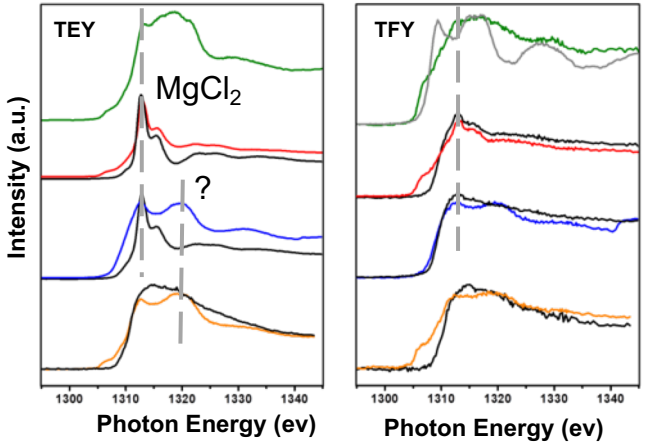

***TEY: penetration depth: ~5nm *TFY: penetration depth: ~ few micro**

- $MgCl_2$ in 2-g-MBH/$MgCl_2$ is dominantly located on the surface.
- $MgCl_2$ might help to remove the oxygen in the bulk.
- Dehydrogenated 2-g-MBH/$MgCl_2$ in bulk does not show the peak corresponding to B_2O_3!

Sohee Jeong, Jeff Urban / Yi-sheng Liu, Jinghua Guo

ALS ADVANCED LIGHT SOURCE

MOLECULAR FOUNDRY

Accomplishments: 2.C Activation of bonds in hydrides

Understanding B-B bond disruption via additives, morphology changes

The B $2p_{xy}$ intensity arises from the MgB_2 B-B ring. LiH and TiH_2 additives disrupt it.

"low" = 0.25 mole fraction; "high" = 0.47 mole fraction

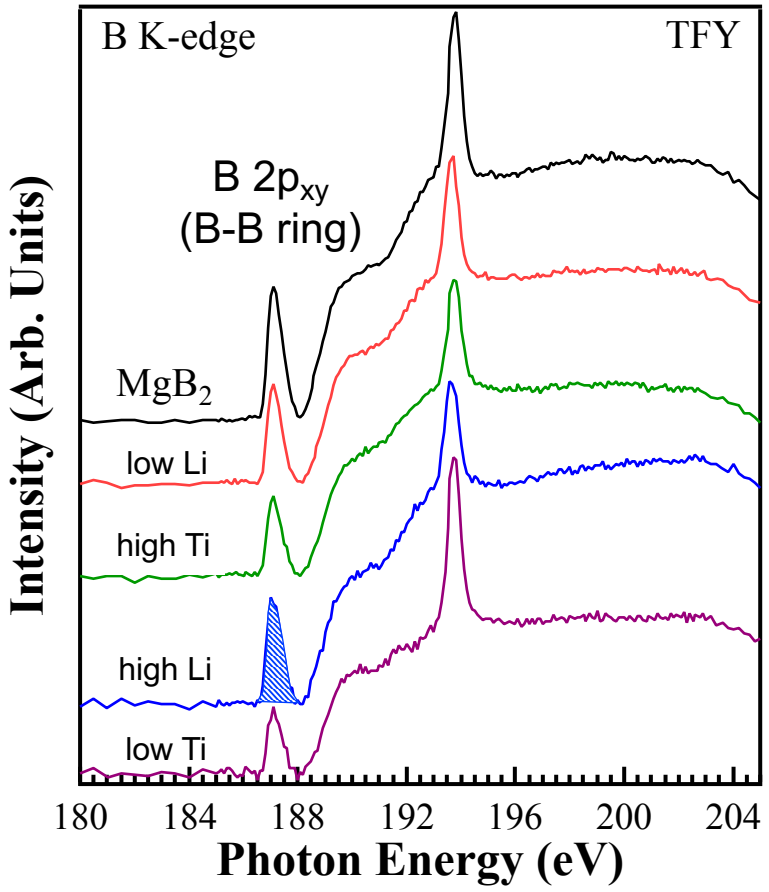

Sample	Integrated B $2p_{xy}$ Area
MgB_2	0.44
MgB_2 + low Li	0.31
MgB_2 + high Li	0.36
MgB_2 + low Ti	0.20
MgB_2 + high Ti	0.25

Both Li and Ti reduce the B-B ring signal, but Ti disrupts it more (predicted by LLNL).

Completed sample characterization by:

- ✓ ***XPS (LBNL)***
- ✓ ***XAS (LBNL)***
- ✓ ***XRD (SNL)***
- ✓ ***FTIR (SNL)***

Approach: We think MgB_2 is hard to hydrogenate because of the stability of the B-B ring. Use additives to disrupt the B-B ring and see if hydrogenation improves.(in progress).

Accomplishments: 2.C Activation of bonds in hydrides

Understanding B-B bond disruption via additives, morphology changes

The morphology of MgB_2 can be affected through surfactant ball milling, producing nanosheets of higher reactivity with H_2.

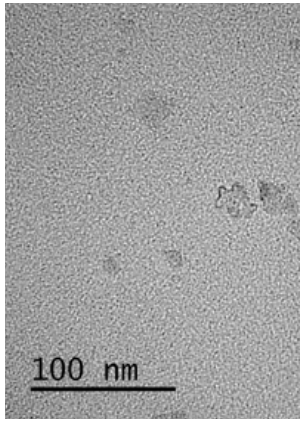

Oleate-bound nanoplatelets

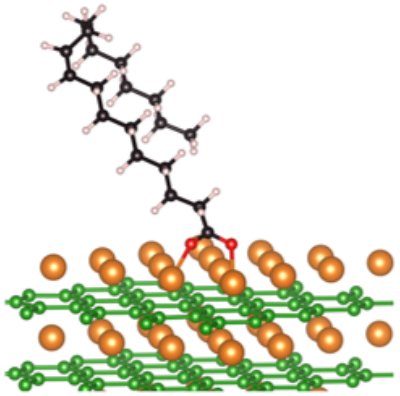

Theory predicts oleate binding motif, properties

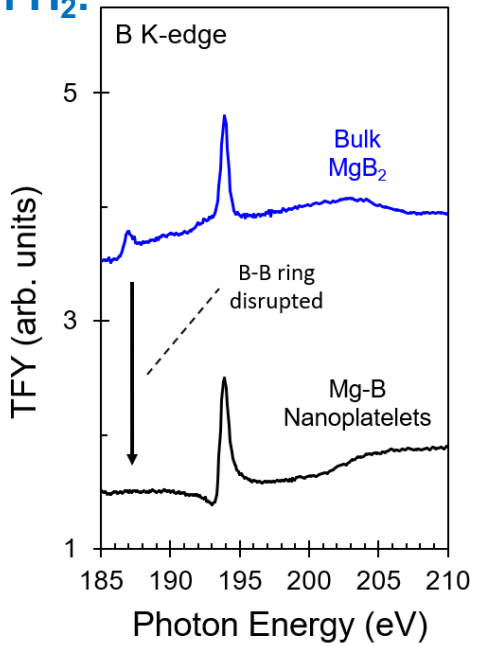

B K-edge XAS reveals the disruption of the B-B ring in the nanoplatelets.

	Lattice Distortions Compared to Bulk MgB_2
In B-B plane, a (Å)	3.122 (+1.23 %)
□ to B-B plane, c (Å)	3.363 (-4.51 %)

XRD indicates lattice distortions from Bulk MgB_2, expanded within B-B nanosheets, contracted between them.

The Mg-B nanoplatelet material forms $[BH_4]^-$ a full 100 ºC below the threshold for MgB_2 hydrogenation at 700 bar.

Next Step: *Try to produce distorted Mg-B material without surfactant*

ARIES: Angle-Resolved Ion Energy Spectrometer

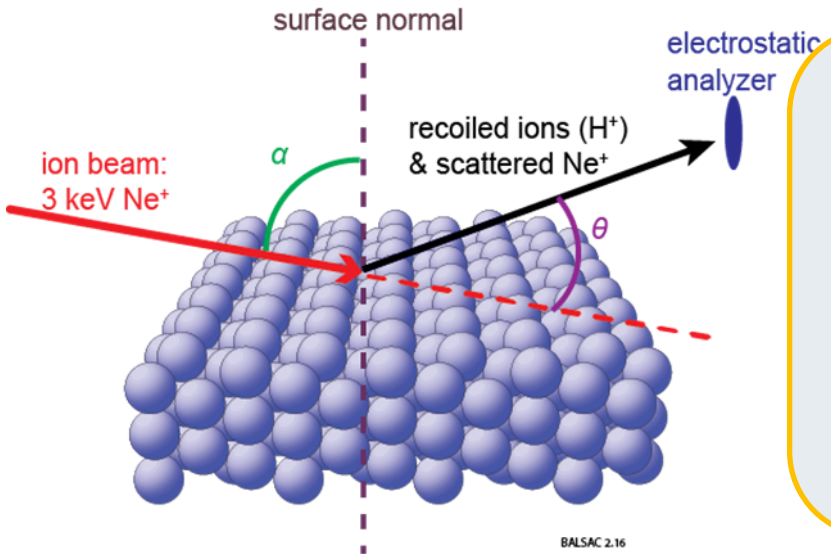

Ion beam (Ne^+) is incident on surface at a glancing angle

Electrostatic analyzer detects ions:

- scattered Ne^+ (LEIS, low energy ion scattering)
- recoiled ions (DRS, direct recoil spectroscopy)

Energy of detected ions depends only on masses and θ, providing surface composition information

Key advantages of LEIS and DRS:

- Extreme surface sensitivity—first monolayer and adsorbates
- Direct detection of surface hydrogen (challenging for most surface science techniques)
- In-situ monitoring of surface in well-controlled environment (~10^{-10} Torr, temperature control)

ARIES surface evolution in $Mg(BH_4)_2$

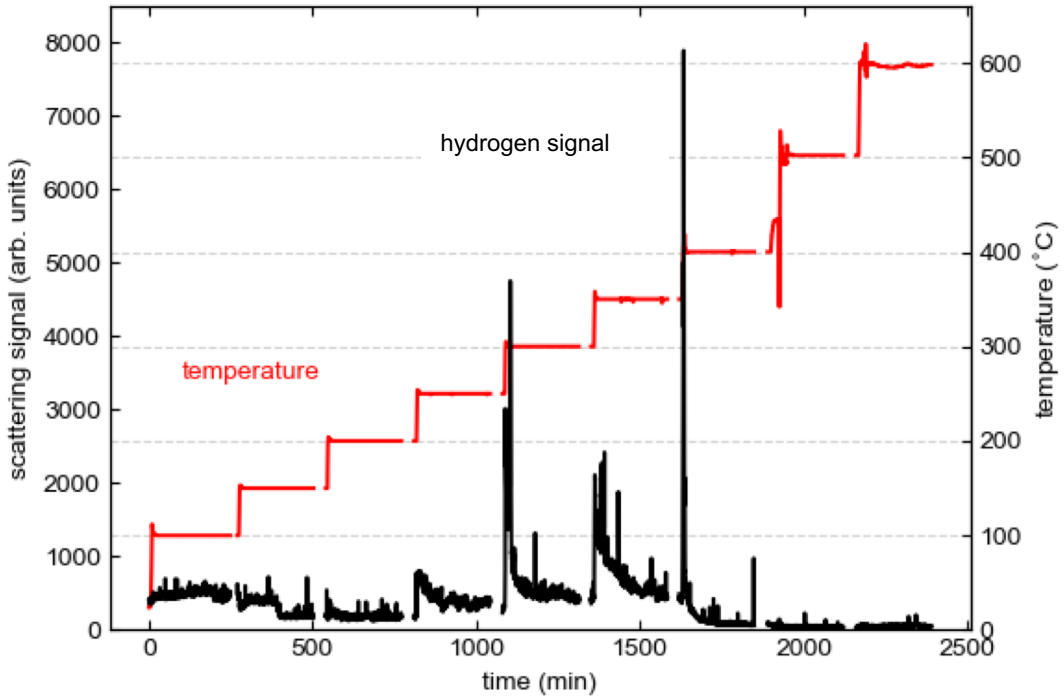

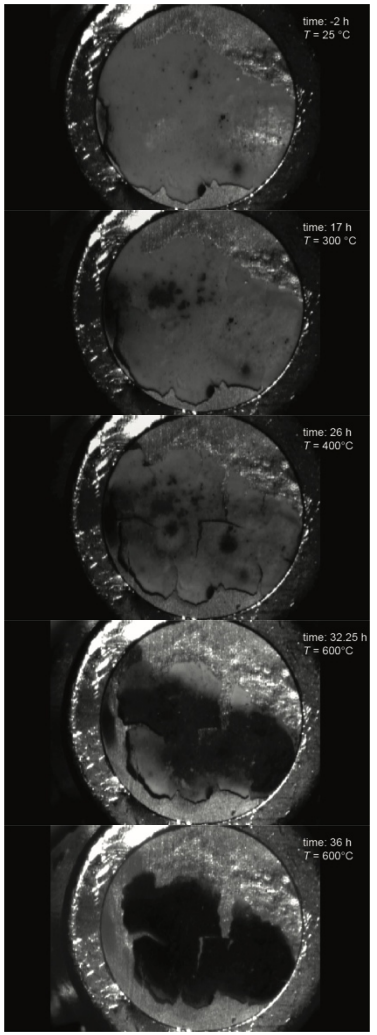

Measurement of surface H with ARIES during the thermal decomposition of $Mg(BH_4)_2$ pressed onto a gold foil:

H segregated to surface mostly at 250-300 ° C and 350-400 ° C, in good agreement with TPD measurements in the literature [1]

[1] Soloveichik et al., Int. J. Hydrogen Ener., (2009).

MD method for predicting H-diffusion in Mg and MgH_2

Predicted Arrhenius Plots

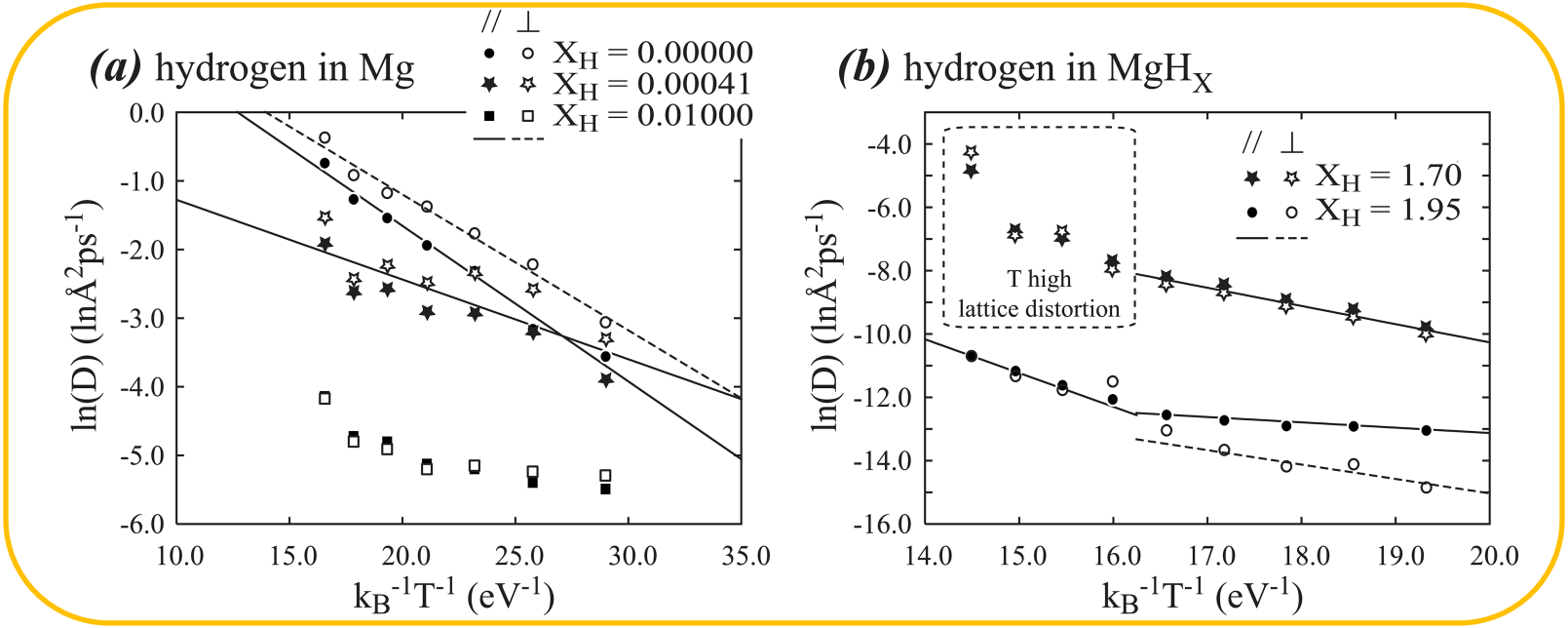

1. Joint SNL-LLNL effort to develop validated models of H-diffusion in Mg.
2. Experiments at given composition/phase cannot relate the diffusivities to hydrogenation state. Hydrogen atoms diffuse vastly faster in Mg metal compared to Mg hydride.
3. Simulations reveal predicted barriers of 0.22 eV in Mg and 1.1 eV in MgH_2, values which agree with the 0.25 eV and 1.1 eV experimental values.

Sandia National Laboratories

Focus Area 2.D.2: Non-innocent hosts for metal hydride nanoencapsulation

$LiAlH_4$ confinement within N-functionalized porous carbons

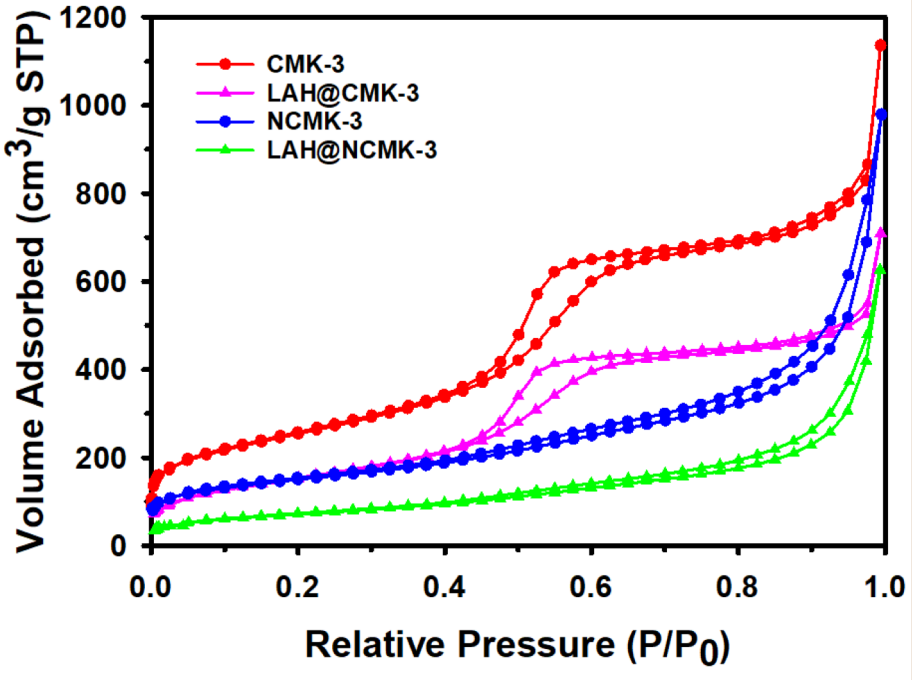

Nitrogen adsorption/desorption isotherms at 77 K of $LiAlH_4$ infiltrated mesoporous carbon scaffolds

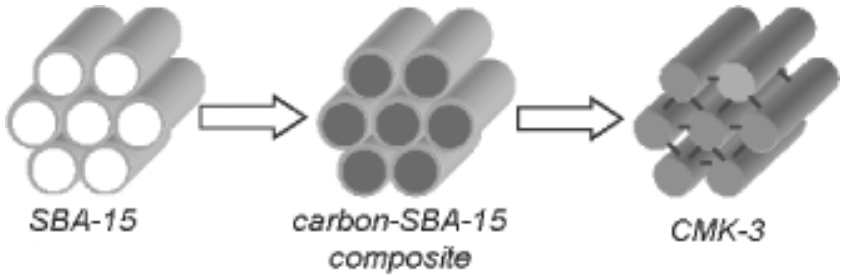

Sample	BET surface area ($m^2\ g^{-1}$)	Total volume ($cm^3\ g^{-1}$)
CMK-3	911	1.76
LAH@CMK-3	560	1.10
NCMK-3	534	1.51
LAH@NCMK-3	261	0.97

Summary of calculated BET surface area and total pore volumes with nitrogen adsorption / desorption isotherms

⇒ Successfully synthesized lithium alanate nanoparticles confined in CMK-3 carbons

Hydrogen release from nanoconfined $LiAlH_4$

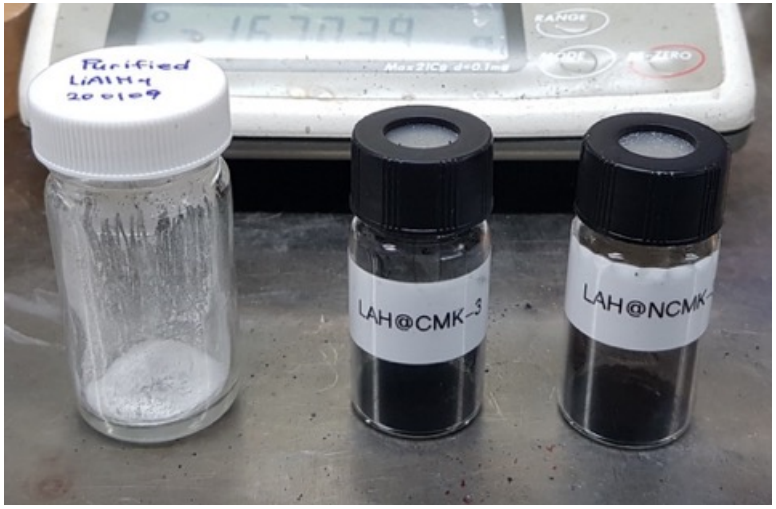

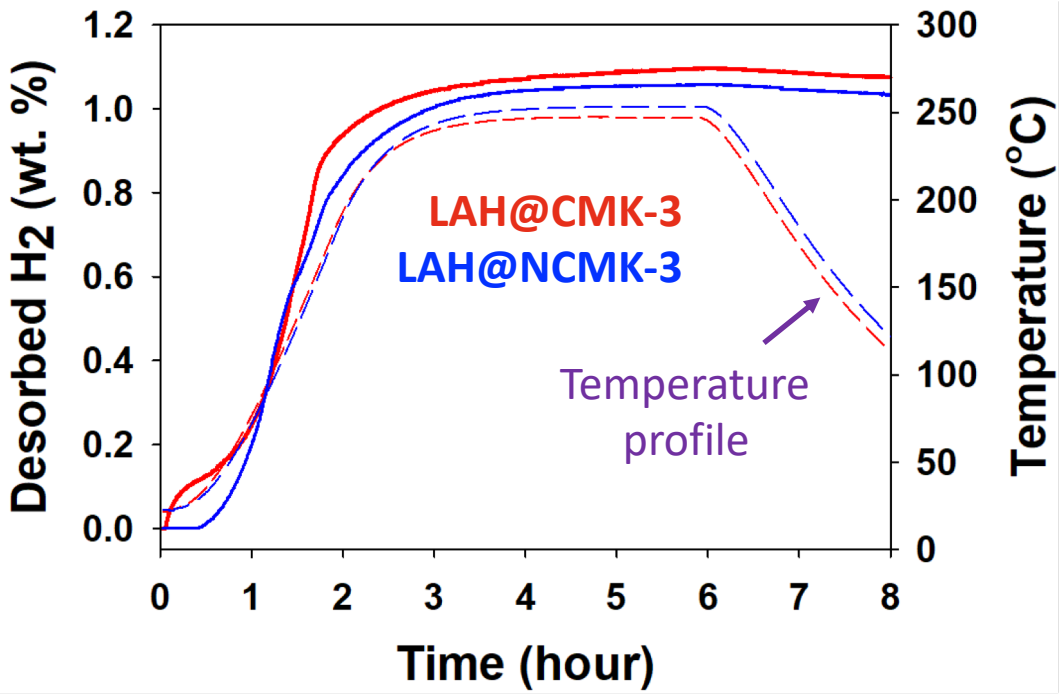

⇒ The nanoconfined materials display fast kinetics of hydrogen release, and the volatiles are mostly composed of hydrogen gas and trace amounts of diethylether

⇒ ^{27}Al MAS NMR indicate that upon desorption the $LiAlH_4$@NCMK-3 and the $LiAlH_4$@CMK-3 samples form LiH and Al bypassing the stable Li_3AlH_6 phase.

Nitrogen doping enables partial reversibility in nano-$LiAlH_4$

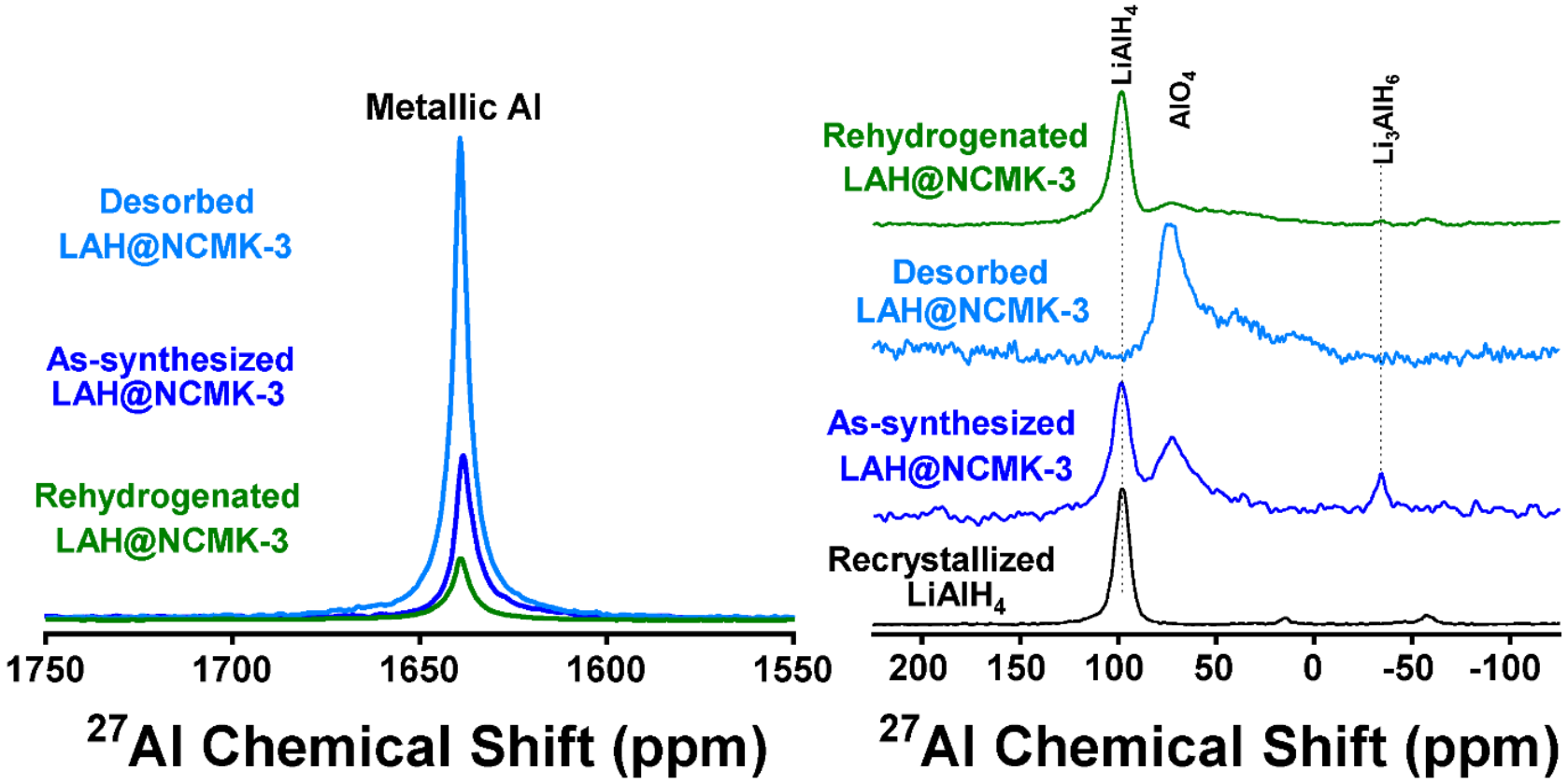

⇒ The MAS NMR results indicate $LiAlH_4$ decomposes at a relatively low temperature
⇒ The conditions for rehydrogenation are 1000 bar hydrogen pressure and 50 ° C
⇒ Only lithium alanate confined in N-doped CMK-3 shows partial reversibility

TEM and EDS measurements

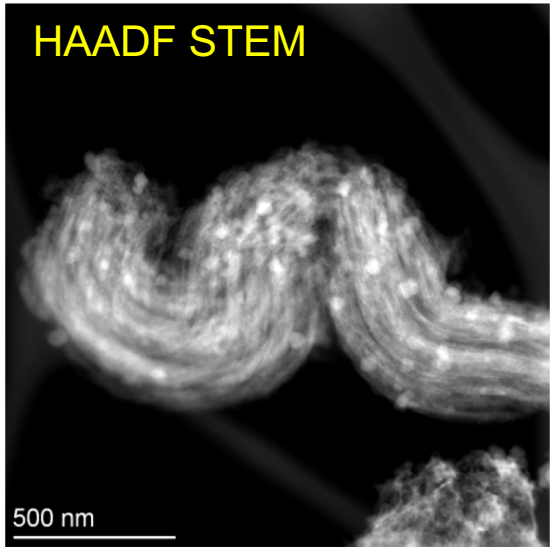

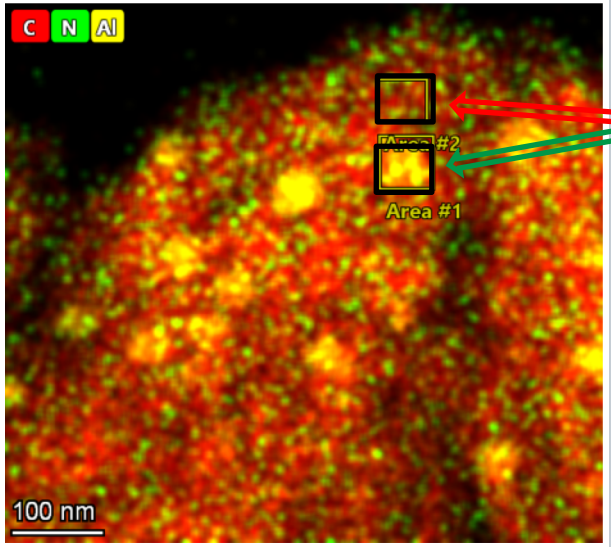

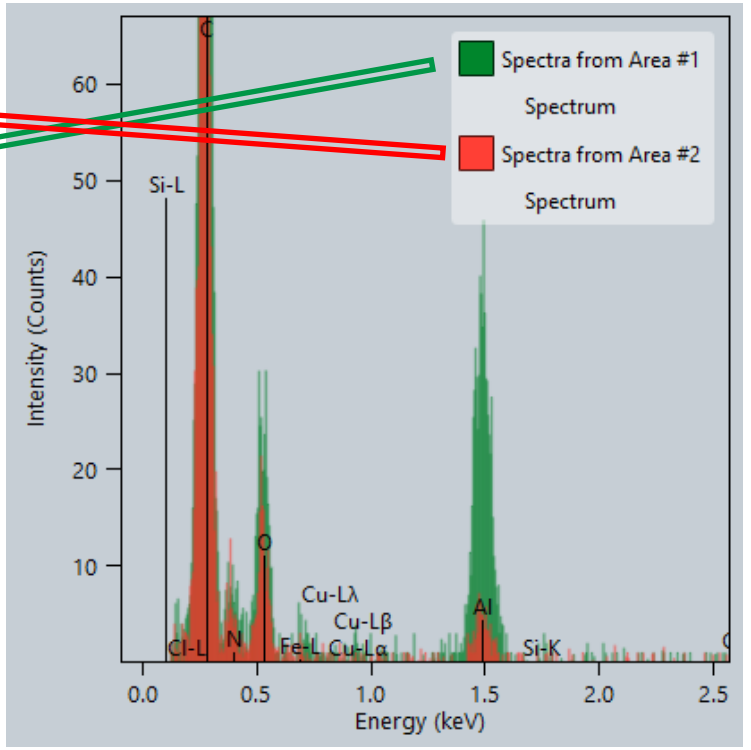

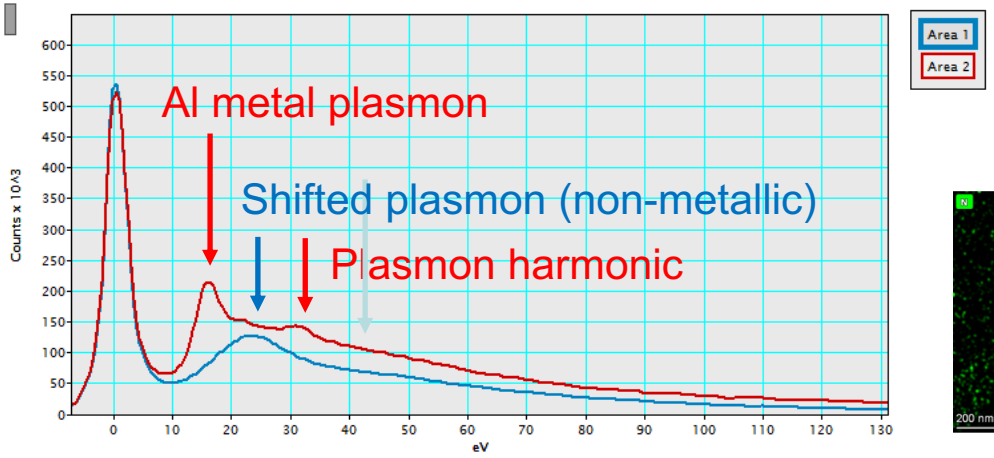

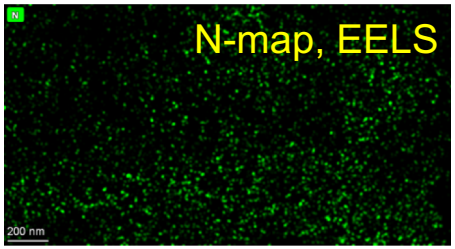

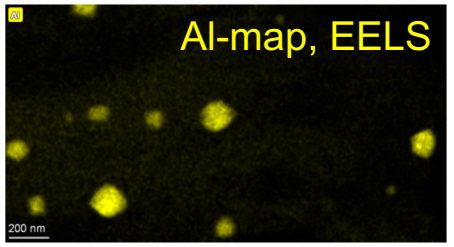

⇒ STEM images of rehydrogenated $LAlH_4$@NCMK-3 showing the distribution of Al species

⇒ EELS spectra and maps confirm the presence of metallic Al (plasmon peak at 15 eV and the harmonic that occurs at 2x15=30 eV), as well as alanate particles (plasmon peak at 24 eV).

Enhanced thermal conductivity of Li_3N@6nm-Carbon

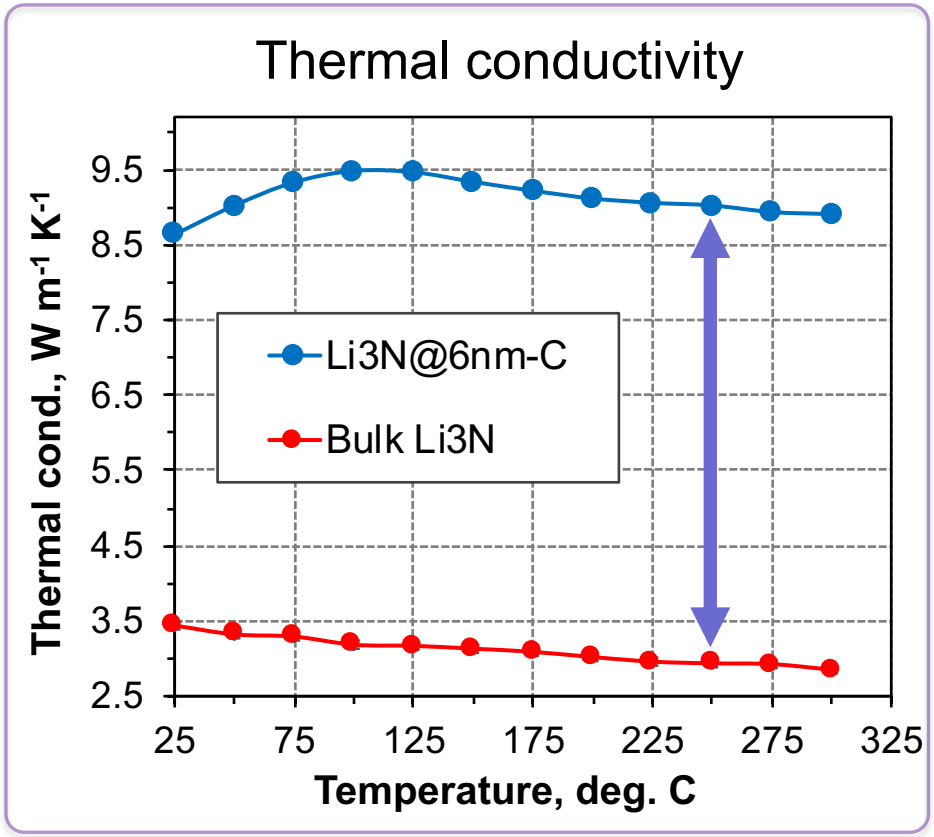

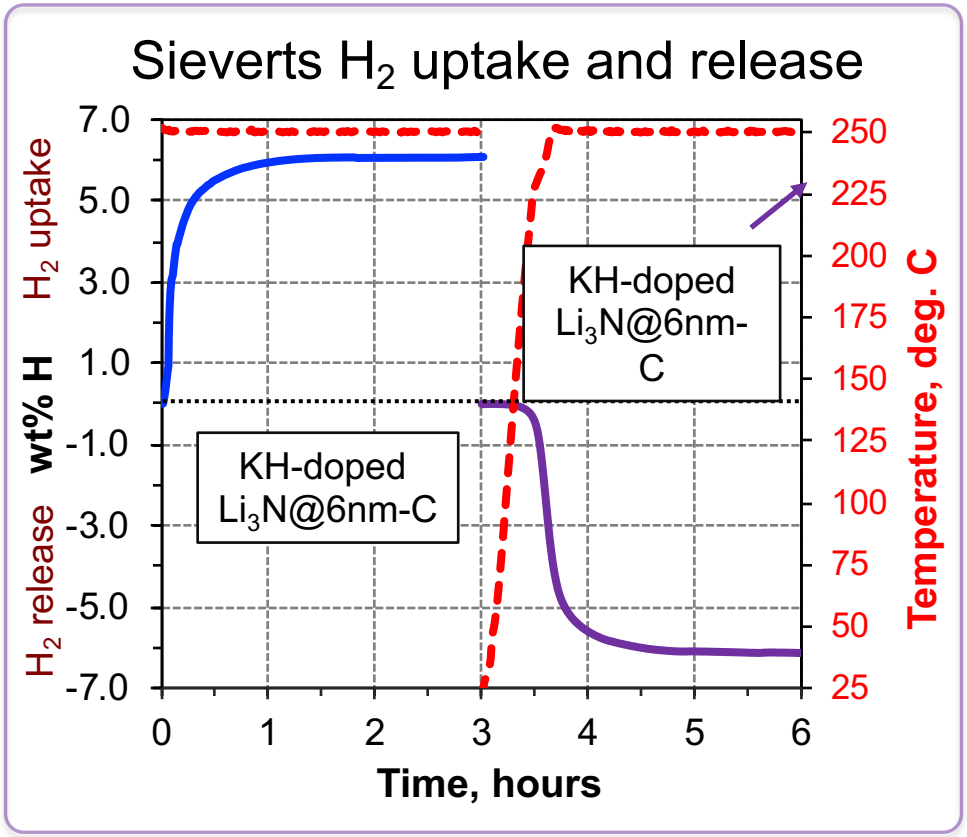

- **Thermal conductivity of nanoconfined KH-6nm-Li_3N@Carbon material is about 2.9-3.2 times higher compared to that of bulk Li_3N**
- **The material can be reversibly cycled at 250 ˚C and 10.5 MPa H_2**

Systems analysis on Li_3N@6nm-Carbon

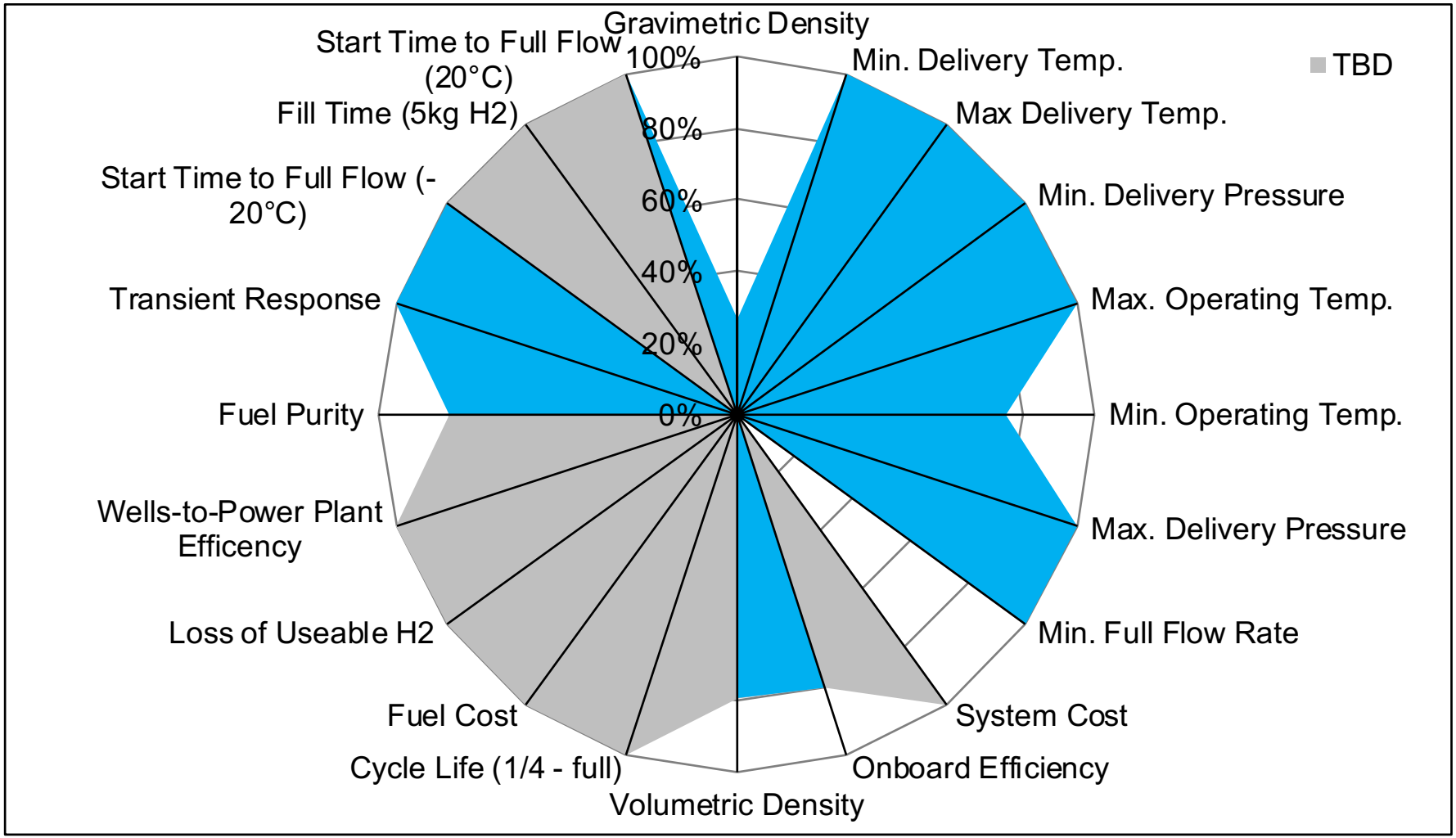

⇒ Finite element analysis reveals that several nanoscale metal amide/nitride materials are closer to meeting the DOE targets compared to bulk materials

Focus Area 2.F Development of machine-learning to discover new metal hydrides

Decades of research on metal hydrides has failed to identify any that meet all DOE targets. Are we missing something?

Research Question: Can machine learning (ML) yield physics-based insight to facilitate the design of novel metal hydrides exhibiting targeted thermodynamic properties ?

Approach:

1. Train an ML model to predict the equilibrium plateau pressure, P_{eq}, of a metal hydride
2. Utilize the ML model's *interpretability* to understand the underlying structure-property relationships from which P_{eq} can be predicted
3. Apply these structure-property relationships to *a priori* identify known intermetallic compositions with unknown hydrides *and* are predicted to exhibit a desired P_{eq}

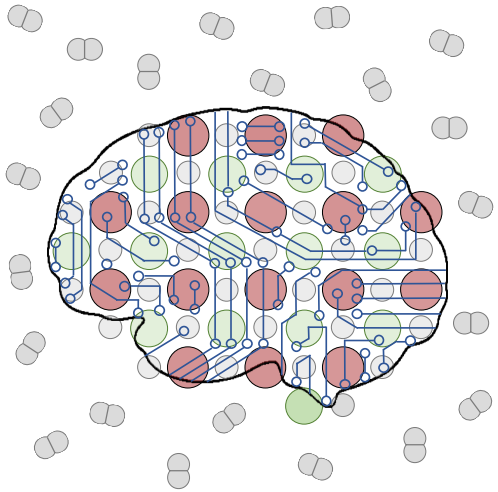

The experimental HYDPARK database contains alloy compositions and the thermodynamics of their hydriding reactions such as ΔH, $\{P_{eq}, T\}$, and H wt. %

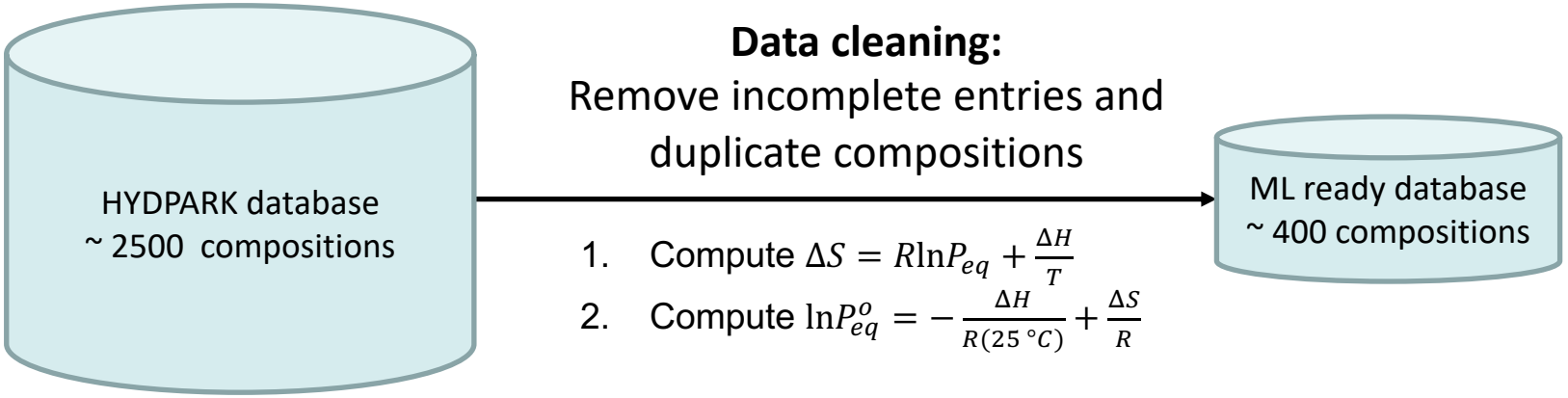

Comp.	ΔH	P_{eq}	T	…
$LaNi_5$				
…				
Er_6Fe_{23}				
…				
…				

Comp.	ΔH	P_{eq}	T	…	$\ln P^{o}_{eq}$
$LaNi_5$					
…					
Er_6Fe_{23}					

We created input features and chose an ML technique that promotes interpretability of the trained model to aid subsequent efforts in rational materials design

Features: each composition (a string) is mapped to a 145 dimensional vector computed from elemental properties using the Magpie code*

Model: Gradient Boosting Trees are interpretable, i.e. they rank how important each feature is to the property prediction

Prediction: $\ln P_{eq}^{o}$

	1	2	v_{pa}^{Magpie}	...145
LaNi5				
…				
Er6Fe23				

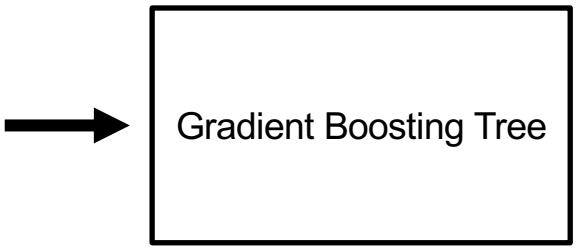

	$\ln P_{eq}^{o}$
LaNi5	
…	
Er6Fe23	

* Developed by Wolverton and coworkers

An example Magpie descriptor:

$$v_{pa}^{Magpie} = \sum_{i} x_i v_i$$

$x_i \equiv$ composition fraction of element i

$v_i \equiv$ ground state volume per atom of elemental solid *i*

ML model can predict lnP_{eq}^{o} with acceptable accuracy using input features derived from only the intermetallic composition

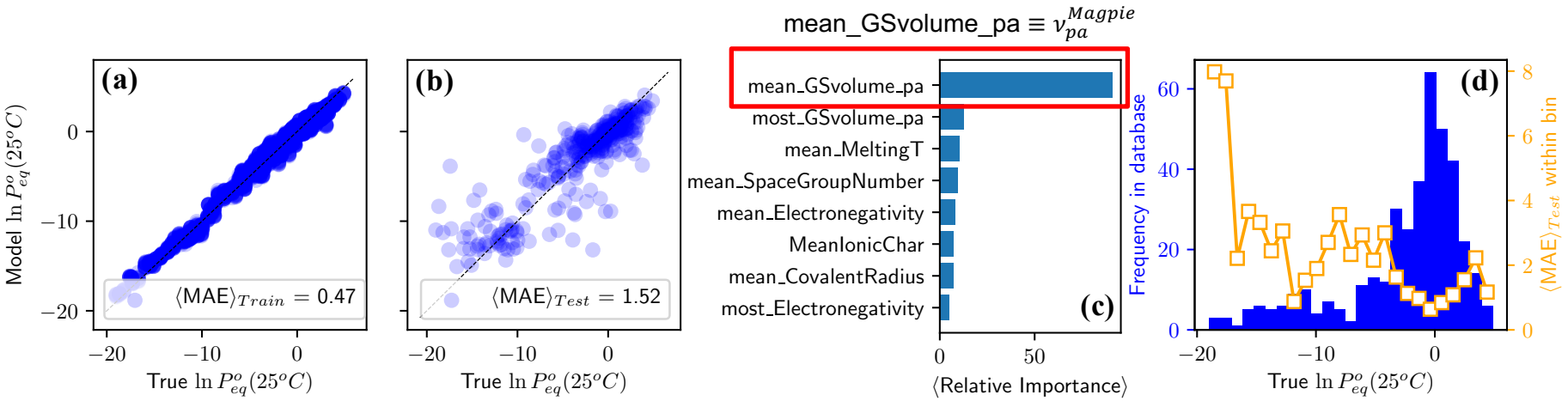

(a), (b) Model validation (test) error as quantified by the mean absolute error (MAE)

(c) mean_GSvolume_pa (v_{pa}^{Magpie}) = Mean ground state volume of the unit cell (approximates volume/atom in the crystal) is the most important Magpie feature

(d) Materials poorly predicted by the model are due to a large imbalance in the distribution of lnP_{eq}^{o}

Our data-driven approach reveals that the ν_{pa}: lnP^{o}_{eq} structure:property relationship is valid for a wide range of metal substitutions and intermetallic classes

1. Compute the structurally specific volume per atom for ~ 70 available structures in the Materials Project (MP) via:

$V_{cell} \equiv$ Volume of the intermetallic lattice computed in MP

$\nu_{pa}^{MP} = V_{cell}/n_{atoms}$

2. Investigate equilibrium pressure as a function of ν_{pa}^{MP} and ν_{pa}^{MP}:

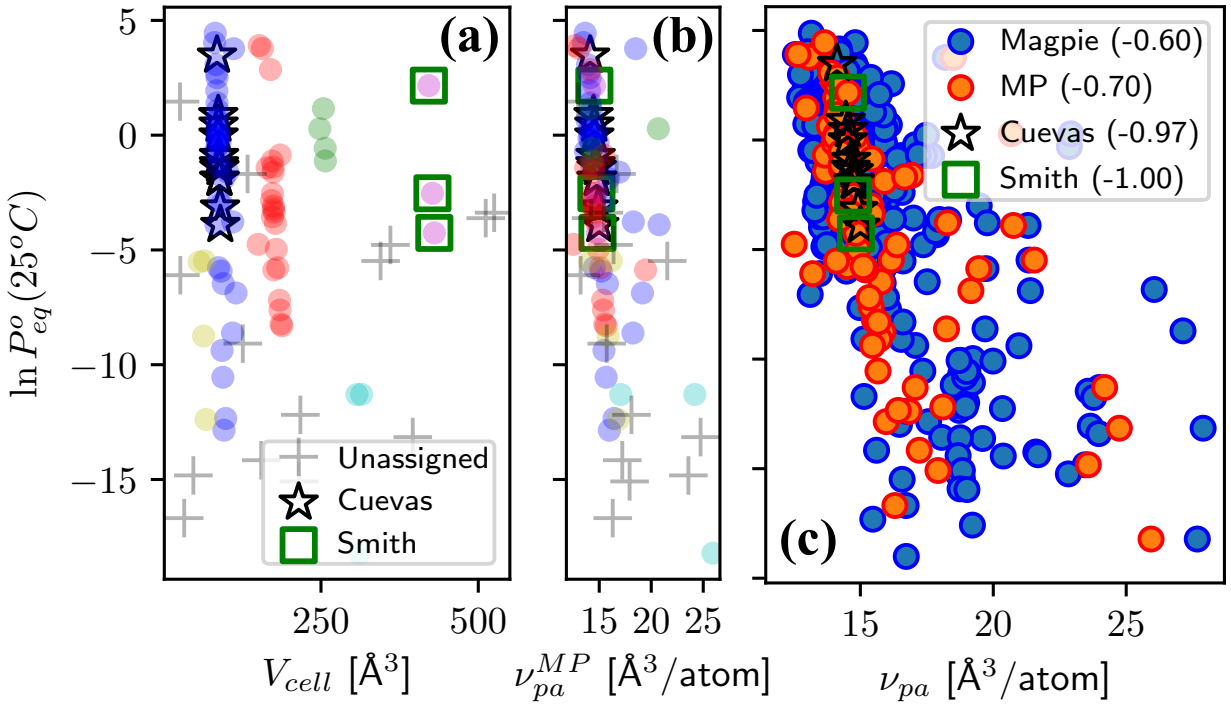

Cuevas et al. noted the dependence of lnP^{o}_{eq} on V_{cell} in $LaNi_5$ substitutions

Smith et al. noted the same trend for R_6Fe_{23} [R=Ho,Er,Lu] substitutions

Utilize this structure-property relationship and DFT validation to propose a novel hydride of a known intermetallic for high-pressure H_2 storage applications

- Known intermetallic compound
- Hydriding properties have been reported
- Would be one of the least stable of all known experimentally reported hydrides

DFT computed properties of the *forward* (hydriding) reaction

	ν_{pa}	ΔH	E_f	ΔE_{def}	ΔE_H	V/V_0
UNi_5	13.17	-0.60	-285	65.2	-65.8	1.278
$CeNi_5$	13.76	-20.5	-353	49.3	-69.8	1.266
$LaNi_5$	14.38	-36.1	-224	44.3	-80.5	1.256

Why does hydride stability tend to increase (lnP^o_{eq} decrease) with increasing ν_{pa}?

1. ΔE_{def} decreases and with it the volume expansion required for hydriding decreases
   ΔE_{def} = energy penalty to deform lattice to accommodate H absorption (kJ/molH_2)

2. ΔE_H [kJ/molH_2] (binding energy of H) tends to become more favorable

3. Together, these two effects lead to a decrease in ΔH [kJ/mol H_2], indicative of a more stable hydride

State-of-the-art PCT with high-pressure calorimeter installed at SNL

Sandia National Laboratories

PCT Pro instrument

- High-accuracy pressure transducers
- Rated up to 200 bar gas pressure and 773 K
- Designed for measurements of H_2 and CH_4 uptake
- Wide range of dosing volumes

Differential scanning calorimeter (DSC)

- SensysEvo instrument from Setaram interfaced through Swagelok connections to the PCTPro
- High-pressure DSC sample holder
  - Rated up to 431 bar gas pressure and 873 K

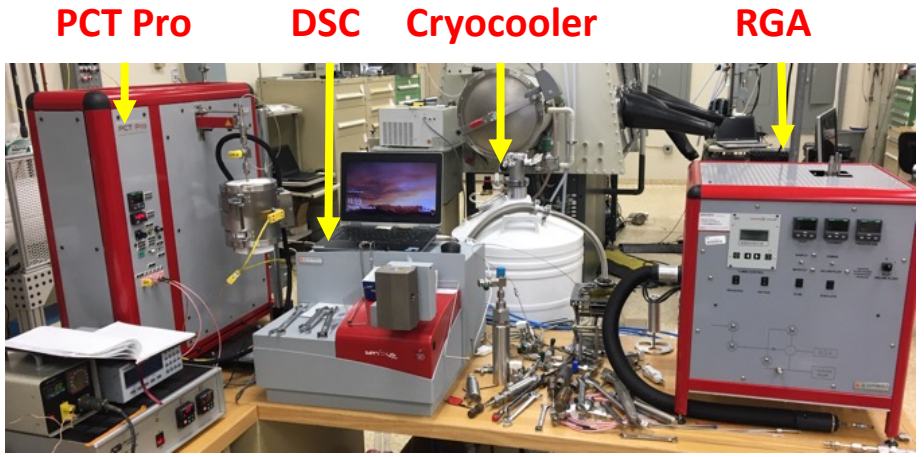

Measured melting point of $Mg(BH_4)_2$ under high-pressure H_2

⇒ The observed heat flow reveals a phase change from the α and γ phases to the high-temperature β phase at ~164 °C.

⇒ A second endothermic peak with a temperature onset at 368 °C and a maximum at 375 °C is assigned to melting of magnesium borohydride just before thermal decomposition

⇒ Integrating the heat flow of the 375 °C peak yields an enthalpy 1.2 kJ·mol^{-1}, which indicates a physical phase change process rather than a chemical reaction.

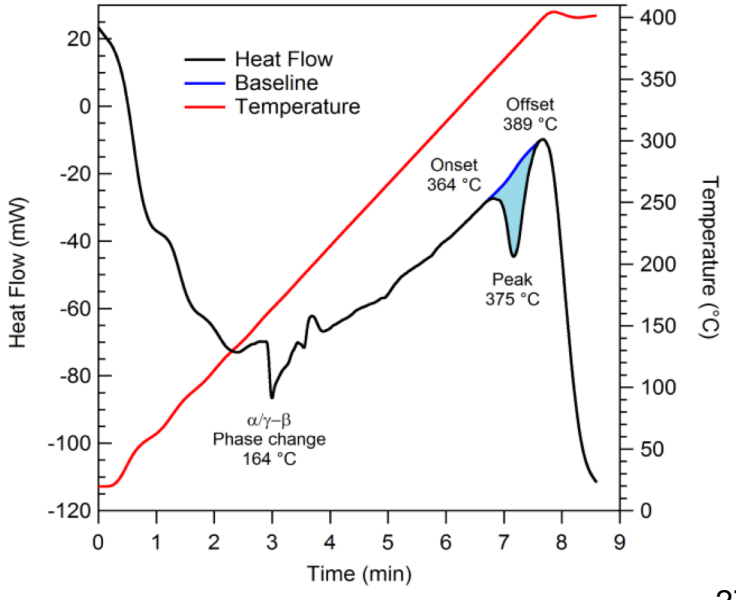

HyMARC currently collaborates with Phase 2 Seedling Projects and facilitating their research on metal hydrides

The HyMARC team assists individual projects with:

- **A designated HyMARC point-of-contact**
- **Technical expertise concerning specific scientific problems**
- **Access to HyMARC capabilities**

- ***Magnesium Boride Etherates as Hydrogen Storage Materials*** (U. Hawaii, G. Severa, Lead)
  - 18 modified MgB_2 samples for ultrahigh-P hydrogenation
  - 12 modified MgB_2 samples for XAS at the ALS

- ***Electrolyte Assisted Hydrogen Storage Reactions*** (LiOx Power, J. Vajo, Lead)
  - 4 samples for ultrahigh-P hydrogenation

- ***ALD Synthesis of Novel Nanostructured Metal Borohydrides*** (NREL, S. Christensen, Lead)
  - 4 samples for ultrahigh-P hydrogenation

HyMARC-NSF seedling projects
FY19 SSMC-EMN Supplemental Funding Opportunity

Tunable Isomorphic Architectures for Hydrogen Storage
Prof. Morgan Stefik, Univ. South Carolina
stefik@mailbox.sc.edu

- Visit by graduate student Eric Williams Nov., 2019
- Synthesis of narrow-pore carbons

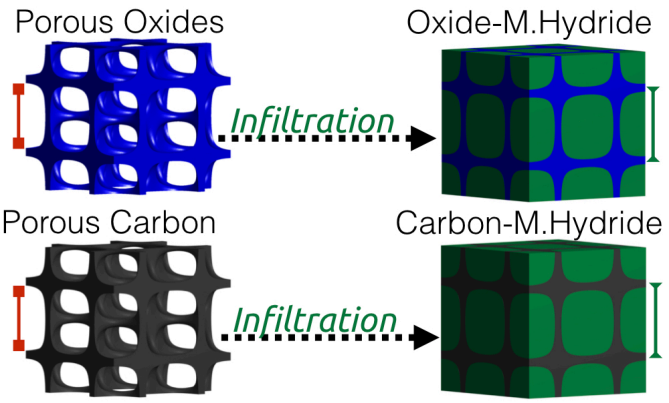

tunable: interface-chemistry, confinement and length scale

Transition Metal-Free Borides for Hydrogen Storage
FY19 SSMC-EMN Supplemental Funding Opportunity
Prof. Viktor Poltavets, Univ. New Orleans
vpoltave@uno.edu

- Visit by grad. student Roshni Bhuvan Oct-Nov 2019
- High-pressure rehydrogenation of doped-MgB_2

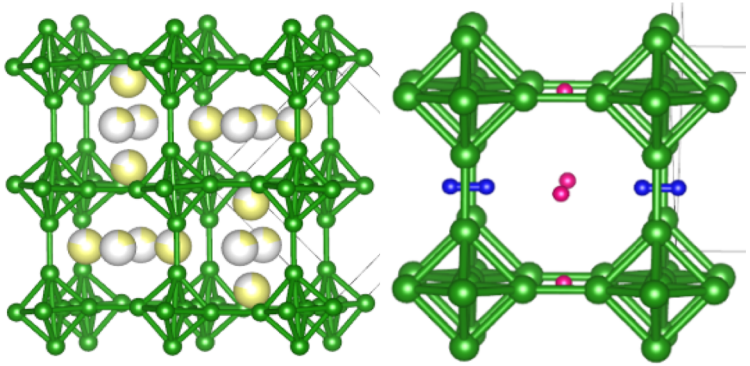

Transition metal doping in MgB_2

Mg-B nanosheets: Collaboration with IIT Gandhinagar (India)

Dissolution of MgB_2

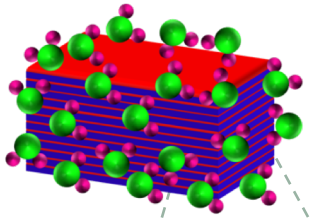

Layered Magnesium diboride crystals in water

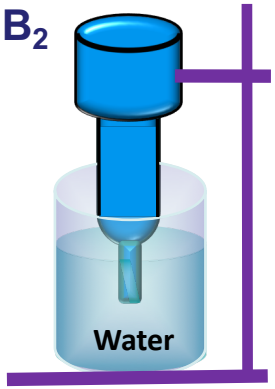

Probe Ultrasonicator

Recrystallization on aging

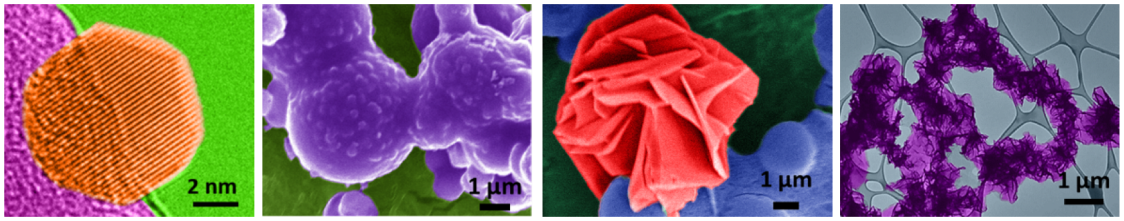

TEM image of nanodot | SEM image of nanograins | SEM image of nanoflakes | TEM image of nanogarland

Characterization of Mg-B nanostructures

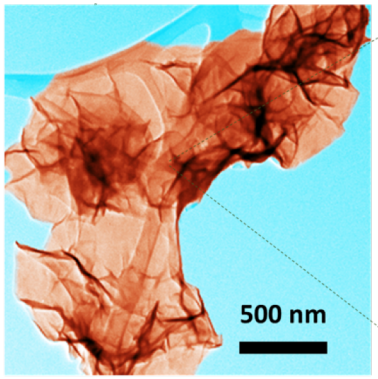

TEM image of a nanosheet

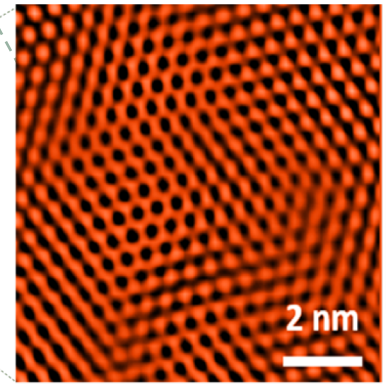

Hexagonal honeycomb network of boron atoms

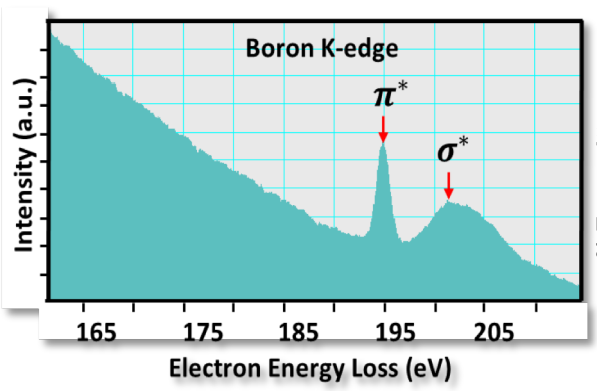

Boron EELS obtained from a nanosheet

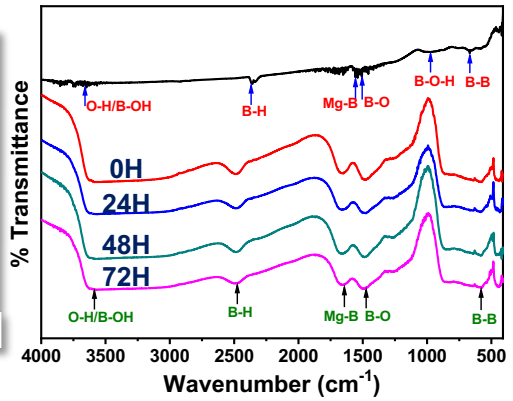

FTIR analysis of nanostructures

⇒ Examining MgB_2 nanosheets to see if they have increased reactivity in hydrogen storage reactions

Sandia National Laboratories | Lawrence Livermore National Laboratory

Exfoliation of MgB_2 in non-aqueous solvents

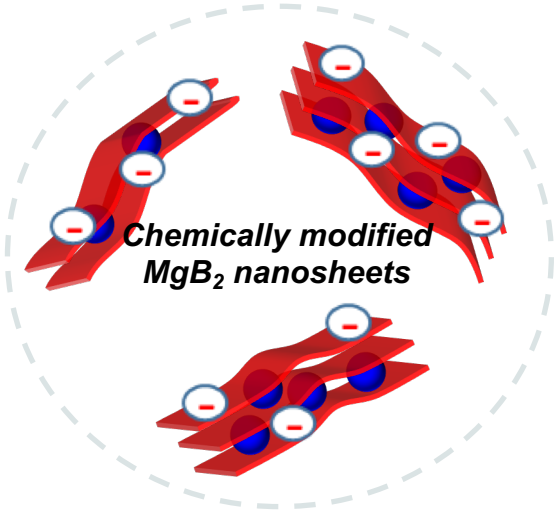

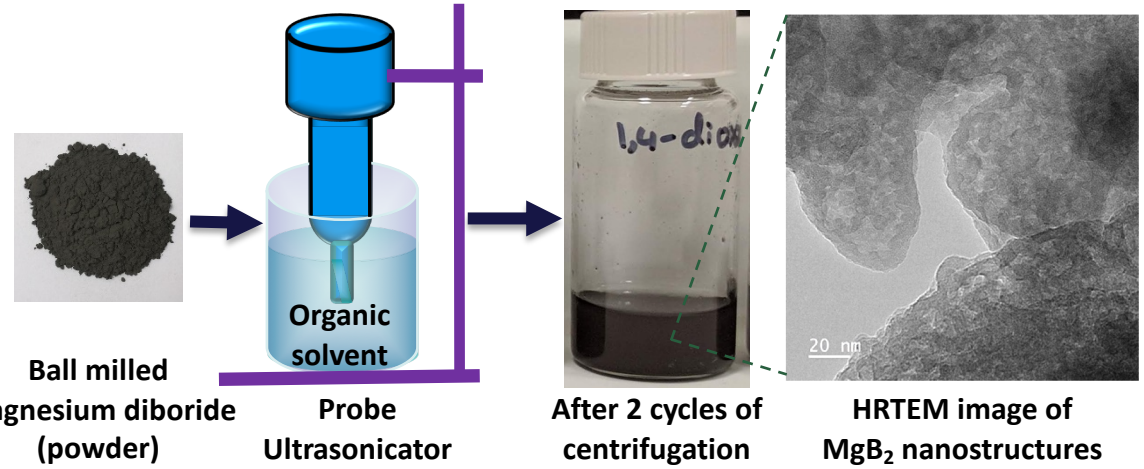

Ball milled Magnesium diboride (powder) | Probe Ultrasonicator | After 2 cycles of centrifugation | HRTEM image of MgB_2 nanostructures

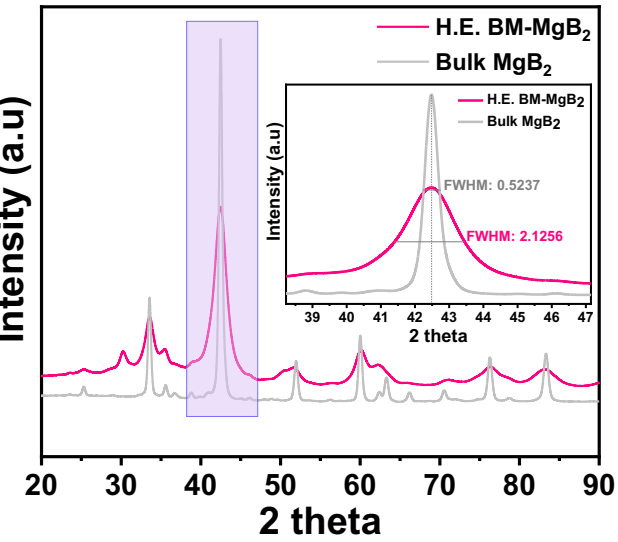

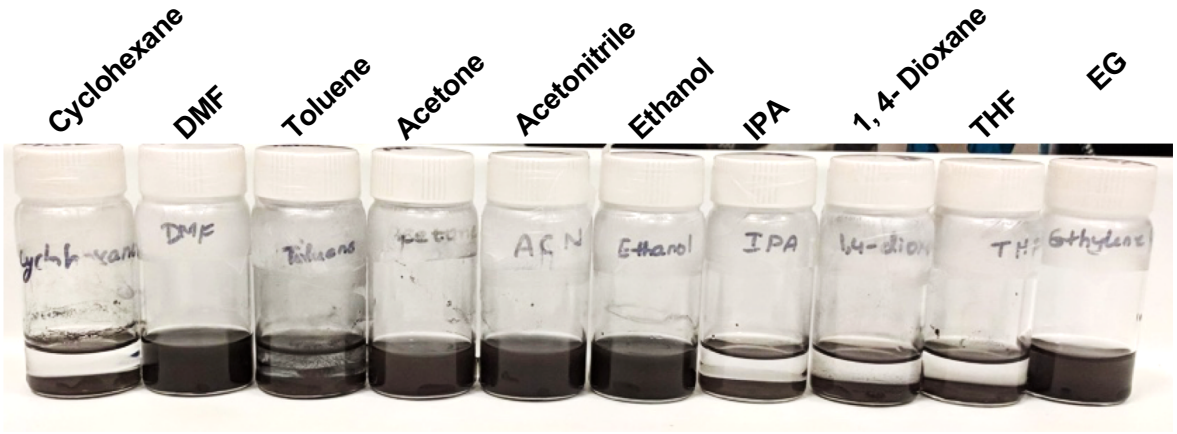

Matching surface energy of MgB_2 and its polar and dispersive component ratios

DMF, ACN, ACETONE, ETHANOL, and EG produce MgB_2 nanostructures

⇒ The ability to create MgB_2 nanostructures depends on the nature of the solvent and surface energy

Sandia National Laboratories | Lawrence Livermore National Laboratory

Collaboration and Coordination

- Timmy Ramirez (Oak Ridge National Lab, USA) : VISION, inelastic neutron scattering
- John J. Vajo, Jason Graetz (HRL Labs, USA): Electrolyte-promoted H_2 storage reactions
- Craig Jensen, Godwin Severa (University of Hawaii): borohydrides for hydrogen storage
- Karl Gross (H_2 Technology Consulting, USA): PCT measurements on metal hydrides
- Morgan Stefik, (University if South Carolina, USA): carbon hosts for nanoconfinement
- Viktor Balema, Vitalij Pecharskij (AMES Lab, USA): metal hydrides, mechanochemistry
- Dhanesh Chandra (University of Nevada, Reno, USA): CALPHAD and phase diagrams
- Dallas Trinkle (UIUC, USA): Predicting hydrogen diffusion in metal hydrides
- Martin Dornheim (Helmholtz-Zentrum Hamburg, Germany): metal hydride composites
- Sanliang Ling (University of Nottingham): DFT calculations and machine learning
- Bettina Lotsch (MPI Festkoerperforschung, Germany): Bypyridine-functionalized hosts
- Torben Jensen (Aarhus University, Denmark): metal borohydrides for hydrogen storage
- Martin Sahlberg (Uppsala University, Sweden): high-entropy alloys for H_2 storage
- David Fairen-Jimenez (University of Cambridge, UK): synthesis of hydride/MOF composites
- Harini Gunda, Kabeer Jasuja (IIT Gandhinagar, India): metal boride nanosheets for H_2 storage
- Shin-ichi Orimo (Tohoku University, Japan): characterization of metal *closo*-borates
- Eun Seon Cho (KAIST, South Korea): strain-induced destabilization of metal hydrides

Publications and Presentations

Selected Papers:

- J.L. White, N.A. Strange, J.D. Sugar, J.L. Snider, A. Schneemann, A.S. Lipton, M.F. Toney, M.D. Allendorf, V. Stavila, "Melting of Magnesium Borohydride under High Hydrogen Pressure: Thermodynamic Stability and Effects of Nanoconfinement" *Chemistry of Materials*, accepted (2020)
- A. Schneemann, L.F. Wan, A.S. Lipton, Y.-S. Liu, J.L. Snider, A.A. Baker, J.D. Sugar, C.D. Spataru, J. Guo, A.S. Autrey, M. Jørgensen, T.R. Jensen, B.C. Wood, M.D. Allendorf, and V. Stavila, "Limit of nanoconfinement? 'Molecular' magnesium borohydride captured in a bipyridine-functionalyzed metal-organic framework," submitted to *ACS Nano* (2020)
- B.C. Wood, T.W. Heo, S. Kang, S. Li, and L.F. Wan, "Beyond idealized models of nanoscale metal hydrides for hydrogen storage" *Ind. Eng. Chem. Res*., **13**, 5786–5796 (2020) [invited article].
- S. Jeong, T.W. Heo, J. Oktawiec, R. Shi, S. Kang, J.L. White, A. Schneemann, E.W. Zaia, L.F. Wan, K.G. Ray, Y.-S. Liu, V. Stavila, J. Guo, J.R. Long, B.C. Wood, and J.J. Urban, "A Mechanistic Analysis of Phase Evolution and Hydrogen Storage Behavior in Nanocrystalline $Mg(BH_4)_2$ within Reduced Graphene Oxide" *ACS Nano*, **14**, 1745–1756 (2020).
- J.L. White, A.A. Baker, M.A. Marcus, J.L. Snider, T. C. Wang, J.R.I. Lee, D.A.L. Kilcoyne, M.D. Allendorf, V. Stavila, FEl Gabaly, "The Inside-Outs of Metal Hydride Dehydrogenation: Imaging the Phase Evolution of the Li-N-H Hydrogen Storage System" *Adv. Mater. Interfaces,* **7**, 1901905 (2020).
- T.W. Heo and B.C. Wood, "On thermodynamic and kinetic mechanisms for stabilizing surface solid solutions" *ACS Appl. Mater. Interf.* **11**, 48487 (2019).
- T.W. Heo, K.B. Colas, A.T. Motta, and L.-Q. Chen, "A phase-field model for hydride formation in polycrystalline metals: Application to δ-hydride in zirconium alloys," *Acta Mater.* **181**, 262 (2019).
- Y.-S. Liu, L.E. Klebanoff, P. Wijeratne, D.F. Cowgill, V. Stavila, T.W. Heo, S. Kang, A.A. Baker, J.R.I. Lee, K.G. Ray, J.D Sugar, and B.C. Wood, "Investigating possible kinetic limitations to MgB_2 hydrogenation", *Int. J. Hydrogen Energy* **44**, 31239 (2019).

Presentations:

37 presentations (3 keynote and 15 invited) at national and International conferences and symposia.

We are grateful for the financial support of EERE/FCTO and for technical and programmatic guidance from Dr. Ned Stetson, Jesse Adams, and Zeric Hulvey

HyMARC
Hydrogen Materials Advanced Research Consortium

Enabling twice the energy density for onboard H_2 storage